

Creep Induced Nonlinear Acoustics in a Ti-Al Alloy

Ti-Al 合金のクリープ損傷中に伴う非線形超音波特性

Toshihiro Ohtani^{1†}, Yutaka Ishii¹, Noritake Hiyoshi² Yasuhiro Yamazaki³, and Yutaro Ohta

(¹Shonan Institute of Technology; ²Fukui University; ³Chiba University; ⁴IHI)

大谷俊博^{1†}, 石井優¹, 旭吉雅健², 山崎泰広³, 太田祐太郎⁴ (¹湘南工大, ²福井大院工, ³千葉大院工, ⁴IHI)

1. Main text

Recently, for higher temperatures and higher efficiency of high-temperature equipment like jet engines and gas turbines, studies of heat-resistant steel and Ni-based superalloys have progressed, and their heat resistance has been greatly improved. In order to further improve the efficiency and reduce their weights, Ti-Al alloy is attracting attention as an advanced heat-resistant material. The microstructure of Ti-Al alloy determined by heat treatment process is affected mechanical properties and strengths¹⁾.

We applied nonlinear ultrasonics for evaluation of creep damage in forged Ti-Al alloy, Ti-43Al-5V-4Nb²⁾. The nonlinear ultrasonics holds the potential of becoming the primary means of characterizing creep in metals³⁾, because it is capable of probing the change of dislocation structure during creep. Its sensitivity to microstructural evolutions during creep is often higher than that of linear properties. We elucidated the relationship between microstructural change and the evolutions of two nonlinear acoustic characterizations; resonant frequency shift⁴⁾, and higher harmonic components⁵⁾ with electromagnetic acoustic resonance (EMAR)⁶⁾ throughout the creep life in Ti-Al alloy.

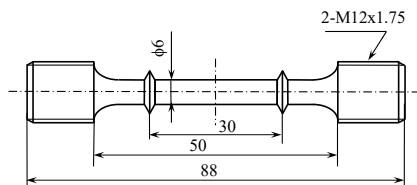


Fig.1 Shape of creep specimen in Ti-Al alloy.

2. Experimental.

The material of the specimens is a forged Ti-Al alloy, Ti-43Al-5V-4Nb. After forging, the microstructure was adjusted by heat treatment. It has a triplex-structure consisted of β -phase, γ -phase and a lamella structure. At room temperature, the mechanical properties are as follows; 0.2% proof stress, $\sigma_y=641$ MPa, tensile strength, $\sigma_B=812$ MPa, and elongation, $\epsilon_f=1.65\%$. Creep specimens with 30mm in gauge length, 6 mm in diameter were cut

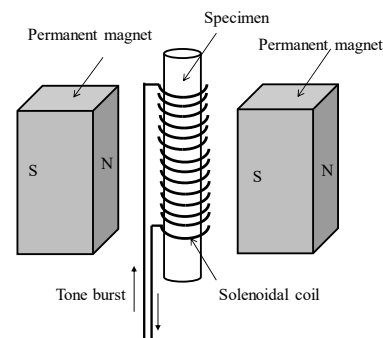


Fig.2 Axial-shear-wave EMAT consisting of a pair of permanent magnets and a solenoidal coil surrounding the cylindrical surface. The Lorentz force causes the axial surface SH wave.

from the forged samples (Fig.1). The creep tests were performed at 923 K in air, and applied stress 380MPa. The rupture life (t_r) was 1,146 h ($\epsilon_f=17.25\%$). Creep tests were interrupted at three creep life ratio at $t/t_r=23\%$, 54%, 83 % (t : creep time, ϵ : creep strain, $t=265.6$ h, $\epsilon=2.1\%$, 622.5h, 5.1%, 955.1h, 10.4%,).

We measured evolutions of the acoustic nonlinearities with the nonlinear resonant ultrasound spectroscopy (NRUS)⁴⁾, and higher components⁵⁾ throughout the creep life with an electromagnetic acoustic transducer (EMAT)⁶⁾. As shown in Fig. 2, we used an axial-shear wave EMAT. Operating of EMAT is referred to Ref 6. The axial shear wave is deflected in the axial direction, and propagates in the circumferential direction.

NRUS analyzed the dependence of the resonance frequency due to the strain amplitude while excitation the specimen at comparative low amplitude. The elastic nonlinearity brings about the resonance frequency shift with increasing the excitation force. By observing the relative frequency shift, it is possible to measure of internal degradation of the microstructural properties of the material. We applied the measurement of NRUS to the EMAR. We defined $\Delta f/f_0$ (resonance frequency shift: Δf , amplitude independent resonance frequency: f_0)⁴⁾ to as the nonlinear acoustic

parameter.

Measurement method of harmonics at the axial-shear wave has shown below ⁶⁾. After driving the EMAT at the fundamental resonance frequency f_1 , we measured the maximum amplitude of the resonance peak, A_1 . We then excited the axial shear wave by driving the EMAT at half of the resonance frequency ($f_1/2$), keeping the input power unchanged. In this case, the driving frequency does not satisfy the resonance condition and the fundamental component does not produce a detectable signal. However, the 2nd harmonic component having double frequency (f_1) satisfied the resonance condition and the resonance spectrum of the received signal contained a peak at the original resonance frequency. We defined this peak height as the 2nd harmonic amplitude, A_2 , to calculate the 2nd harmonic nonlinearity A_2/A_1 . We defined the 3rd harmonic nonlinearity, A_3/A_1 , in the same way. We used the systems for a nonlinear acoustic phenomenon (SNAP) manufactured by RITEC.

3. Results and discussions

Figure 3 shows the relationship between the nonlinearity of the 2nd and 3rd harmonics, A_2/A_1 , A_3/A_1 , nonlinearity of NRUS, $\Delta f/f_0$, attenuation coefficient, α (attenuation per unit time), relative velocity, $\Delta V/V_0$ ($\Delta V=V-V_0$, V : velocity, V_0 : initial velocity) in the first resonance mode (around 0.38 MHz), and creep life fraction t/t_r . After slightly increasing from the start to $t/t_r=20\%$, second harmonics, A_2/A_1 , shows tendency of decrease to the rupture (Fig.3 (a)). Third harmonics, A_3/A_1 , $\Delta f/f_0$ and α show the same as tendency of the second harmonics (Figs.3 (b) (c) and (d)). $\Delta V/V_0$ decreases from the start to $t/t_r=20\%$. Then, they gradually increased to rupture. The increment was around 5%. In metals, possible factors contributing to non-linear acoustics during creep are as follows ⁶⁾: (i) nonlinear elasticity due to lattice anharmonicity (ii) inelasticity due to dislocation movement and (iii) crack opening and closure when an acoustic wave impinges on the crack faces. Therefore, (i)-(iii) explains the observed nonlinearity during creep. These first two factors are inseparable in actual nonlinear measurement. From accordance with the trends of A_2/A_1 , A_3/A_1 , $\Delta f/f_0$ and α during creep in Fig.3, we considered that the evolution of non-linearity results from the dislocation multiplication until $t/t_r=20\%$ and the recovery and recrystallization by creep from $t/t_r=20\%$. Nonlinear acoustic characterizations with EMAR were able to detect microstructural change throughout the creep life in the forged Ti-Al alloy, Ti-43Al-5V-4Nb. In the future, we plan to observe the microstructure related to changes in nonlinear acoustics.

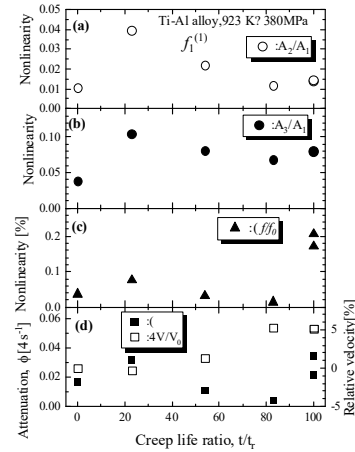


Fig. 3 Evolutions of (a) the nonlinearity in 2nd harmonics, (b) the nonlinearity in 3rd harmonics, (c) the nonlinearity with NRUS and (d) attenuation coefficient and relative velocity in Ti-Al Alloy during creep (923 K, 380 MPa, $t_r=1,146$ h).

4. Conclusion

The high sensitivity and contactless aspects of EMAR enabled the precise measurement of two nonlinear acoustics; resonant frequency shift and higher harmonic components throughout the creep life in the forged Ti-Al alloy, Ti-43Al-5V-4Nb. Two nonlinear acoustic parameters and ultrasonic attenuation increased from the start to 20% of creep life. Then, they rapidly decreased to rupture. We interpreted these phenomena in terms of dislocation mobility and restructuring.

Acknowledgment

This work was performed as a part of the collaborative study in the committee on Titanium-Aluminide alloy, the Society of Materials Science, Japan.

References

1. R. J. Lancaster, S.P. Jeffs, H.W. Illsley, C. Argyrakis, R.C. Hurst and G. J. Baxter, Mater. Sci. Eng. A **748**, (2019),21.
2. Y. Yamazaki, R. Sugaya, U. Kobayashi, and Y. Ohta, Mater. Sci. Eng. A. **797**(2020), 140248.
3. K. Y. Jhang, Inter. J. Precision Eng. & Manufacturing **11** (2009), 123.
4. K. E-A Van Den Abeele and J. Carmeliet, Res. Nondestructive Eval. **12** (2000) 31.
5. A. Hikata, F.A. Sewell Jr., and C. Elbaum, Phys. Rev. **151**(1966) 442.
6. M. Hirao and H. Ogi, EMATs for Science and Industry: Nondestructive Ultrasonic Measurements, (Kluwar Academic Publishers, 2003), p1.